Impact Ice Stresses in Rotating Airfoils

R. J. Scavuzzo,* M. L. Chu,† and C. J. Kellackey‡
University of Akron, Akron, Ohio 44325

Under adverse conditions, impact ice can accumulate rapidly on rotating airfoils such as helicopter blades, propellers, and tail rotors. Shedding of impact ice accumulated on these surfaces can cause large unbalanced forces. Because of the statistical variation of the adhesive strength, unbalanced shedding can be expected. It is the purpose of this paper to present two studies of the basic problem. Finite element modeling of the rotating ice-airfoil system was used as the basic tool to study the tensile and shear stresses at the interface between the impact ice and metal airfoil surface. Two models were developed. The first model was a simple rotating beam-ice structure used to obtain a basic understanding of stress distribution in the ice. Calculations show that shear stresses increase linearly with the ice thickness and tensile stresses tend to zero for a fully bonded surface. When shear stresses exceed the ultimate strength, adhesive failure occurs and tensile stresses are developed in the unbonded ice. Tensile failure of the impact ice results. In the second finite element study the OH-58 tail rotor was modeled with a measured ice profile. The rotor was tested in the icing research tunnel (IRT) at the NASA Lewis Research Center. Predictions of ice shedding are compared to this data using a statistical structural analysis.

Introduction

EARLY work in the de-icing field by Jellinek[1] suggested that the adhesive strength of snow ice is independent of the cross-sectional area and the thickness of the ice layer. Jellinek also suggested a linear relationship between increasing adhesive strength and decreasing temperature until it becomes larger than the cohesive strength of ice at about $-13°C$ (9°F). He also found that the tensile (cohesive) strength is several magnitudes smaller than expected from theory. While examining different substrate materials, Stallabrass and Price[2] found that ice adheres to Teflon-coated components as strongly as it does to metal components. They also concluded that inadvertent contamination (fingerprints, machine oils, rust, etc.) reduces ice adhesion to metals. They went on to suggest that an application of wax or varnish may reduce adhesion still further. Their results also showed a trend of stronger adhesive strength at lower temperatures. Itagaki[3] investigated the self-shedding of ice from rotating struts and developed a relationship for finding the tensile and adhesive strengths of accreted ice. He found that tensile and adhesive shear strengths show little dependence on temperature, contrary to previous work done. Itagaki's analysis showed higher tensile strength with slower-grown ice, indicating that some strengthening process (such as sintering or recrystallization) occurs during ice accretion. Furthermore, the adhesive shear strength is greater for faster-grown ice.

Scavuzzo and Chu[4] extensively studied the shear strength of rime-glaze ice and its dependence on various conditions. Values were found by the use of two test apparatus that are described in their report. As with all icing research, there was a large amount of scatter in the shear stress values. This study revealed that the adhesive shear strength of the accreted impact ice was statistically independent of the following: 1) tunnel air temperature below 25°F, 2) the thickness of the accreted ice, 3) material substrate, 4) cloud-on cloud-off conditions, 5) rotation or nonrotation of the shear specimen, and 6) the slope of the window of the shear test specimen. (See Ref. 4 for further details.) Their work also concluded that several factors do affect the adhesive shear strength. As surface roughness increases, so does the adhesive strength. Roughness was then held constant as wind velocity, droplet size, and ice surface temperature were varied. The report states that the shear strength increases slightly as the wind velocity and droplet size increase for hard rime-glaze ice; however, the shear strength is not affected by interface surface temperatures below 25°F. Between 25°F and the melting point, there is a linear drop in adhesive shear strength. Additionally, the shear strength was plotted against droplet momentum to show that the strength increases slightly with increasing droplet momentum.

Work done by Druez et al.[5] during the same time also found a large amount of scatter in the adhesive shear strength of ice specimens. Although the data trends are similar between this testing and that done by Scavuzzo and Chu,[4] the magnitude of the values differs greatly due to the difference in wind velocities. It is evident from this work, however, that the adhesive shear strength values for glaze ice are significantly larger than those of the rime ice (approximately twice as large), other conditions being constant. This study also revealed that the shear strength of ice is independent of the rate of deformation.

Recent de-icing work done by Miller and Bond[6] found that ice accretion on rotor blades produces a torque rise that varies linearly with time for a fixed set of rotor and tunnel conditions. It was also found that the torque rise rate is dependent on cloud conditions and temperature. Lower liquid water content and smaller drop size results in a slower torque rise. Furthermore, there is some temperature at which the majority of the ice is glaze and extends to the tip without shedding. Research showed that the torque rose steadily until shedding occurred. At this time, the torque dropped somewhat, but as the ice accretion continued, the torque rose again until another shed occurred. Rotor vibration became a problem when ice shedding occurred asymmetrically. Measurements of rotor blade ice profiles were found to be repeatable, as were the iced rotor torque values, until the onset of shedding for a given set of conditions. Although the test rotor was not able to achieve a rotational speed high enough to obtain shedding on most of the runs, data showed that, when sheds did occur, the radial extent of the nonshed ice was repeatable, but that the shed time, as well as the locations and quantities of ice shed, exhibited large variations from run to run.

The objective of this paper is to present the results of finite element analysis of impact ice adhered to a rotating airfoil. Results are compared to the analysis of Itagaki.[3] In addition,

Received Jan. 6, 1990; presented as Paper 90-0198 at the AIAA 28th Aerospace Sciences Meeting, Reno, NV, Jan. 8-11, 1990; revision received and accepted for publication Aug. 15, 1990.

*Associate Dean, College of Polymer Science and Polymer Engineering. Member AIAA.
†Professor of Mechanical Engineering. Member AIAA.
‡Graduate Research Assistant.

the probability of an ice shed from a test program on a rotor test rig (OH-58 test) in the icing research tunnel (IRT) at the NASA Lewis Research Center is calculated. This statistical structural analysis of OH-58 data is based on stresses calculated by finite element analysis and a statistical analysis of measured impact ice shear strength.[11]

Finite Element Analysis

Shearing stresses in an iced rotating airfoil at the substrate-ice interface are evaluated using finite element methods, and these results are compared to the values calculated with Itagaki's theory.[3] Additionally, the stresses created by an actual ice deposit from the OH-58 tests[6] are calculated. The analytical predictions are made using the COSMOS/M finite element software package.[12] The basic assumption in the following finite element models is that the strains in the rotating airfoil are developed before ice formation begins. Therefore, it is assumed that the airfoil is rotating and then impact ice is accreted. The modeling technique used to simulate this condition assumes that the airfoil structure has zero mass density. Because of this assumption, axial strains in the airfoil structure are caused by the added ice mass only. The ice is not strained by rotational inertia forces. A solid eight-noded element was used in the modeling of both the ice and the structure. Composite elements were considered and discarded because of limitations with the method of mass distribution in the element for dynamic problems. Results from the following analytical models are presented in the following sections.

The simplest analysis of shear stress can be developed assuming that a button of ice with a cross sectional area A is adhered to a rotating airfoil at a radius R. By considering the inertia force on the ice button, the shear stress at the interface can be calculated

$$\tau = \rho\omega^2 Rh \qquad (1)$$

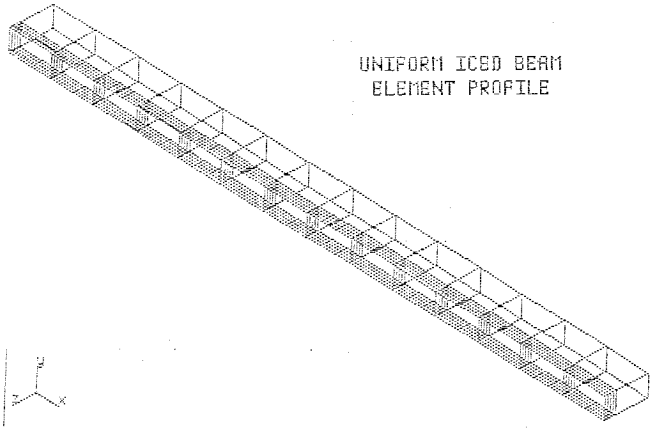

Fig. 1 Finite element model of a uniform continuous iced beam.

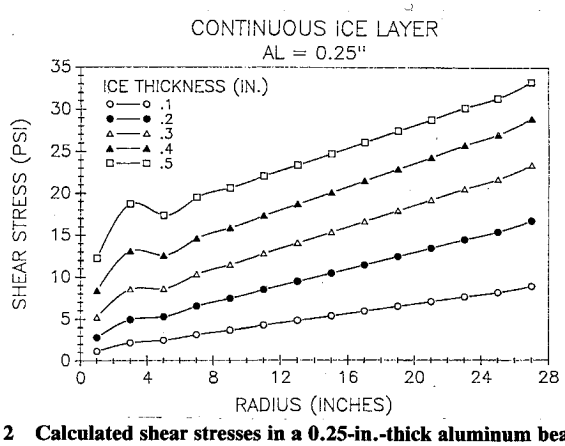

Fig. 2 Calculated shear stresses in a 0.25-in.-thick aluminum beam.

where R is the radial length, ω the angular velocity, ρ the density of ice, and h the ice thickness. As will be shown, finite element results approach this simple equation when the axial stiffness of the airfoil is high compared to that of the ice.

Uniform Ice Layer

A uniform layer of ice was added to the inside edge of a rotating aluminum beam. Figure 1 shows a three-dimensional view of the element profile. At first, the thickness of the aluminum was set at 0.25 in., whereas the ice varied between 0.1 and 0.5 in. Shear and axial normal stress plotted against radial position are shown in Figs. 2 and 3, respectively. However, when the shear values were compared to Eq. (1), there was a large discrepancy because of the axial strain in the aluminum (see Table 1). As a result, the beam thickness was then increased to 1.5 in. and then the elastic modulus was increased to 10^{10}. Plots of shear and normal stress vs radial position can be found in Figs. 4 and 5. As seen in Figs. 4 and 5, the maximum sheer stress approaches the button formula value of 56 psi and the tensile stresses are almost zero.

It can be concluded that this model approaches the button formula equation. The shear stress seems to follow a linear relationship with the maximum shear stress approaching the

Table 1 Shear stress calculations for continuous ice layer model

Ice thickness, in.	Theoretical value (Eq. 2)	FEA[a] value at 27.75 in. (Al = 0.25 in.), psi	FEA value at 27.75 in. (Al = 1.5 in.), psi	FEA value at 27.75 in. (E = 10^{10}), psi
0.1	11.3	8.9	9.4	9.8
0.2	22.6	16.7		
0.3	33.9	23.4		
0.4	45.2	28.9		
0.5	56.4	33.3	43.0	48.4

[a]FEA = finite element analysis.

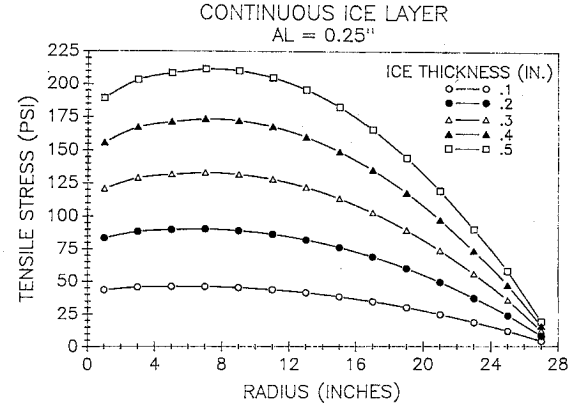

Fig. 3 Calculated tensile stresses in a 0.25-in.-thick aluminum beam.

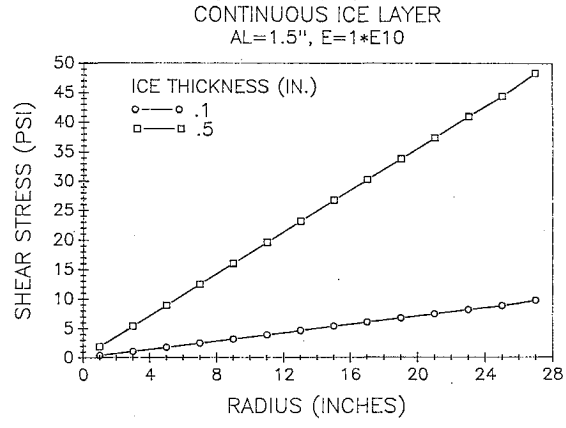

Fig. 4 Calculated shear stresses in a thick rigid beam.

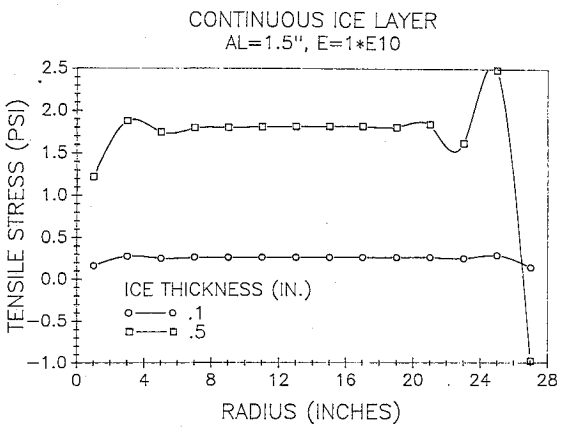

Fig. 5 Calculated tensile stresses in a thick rigid beam.

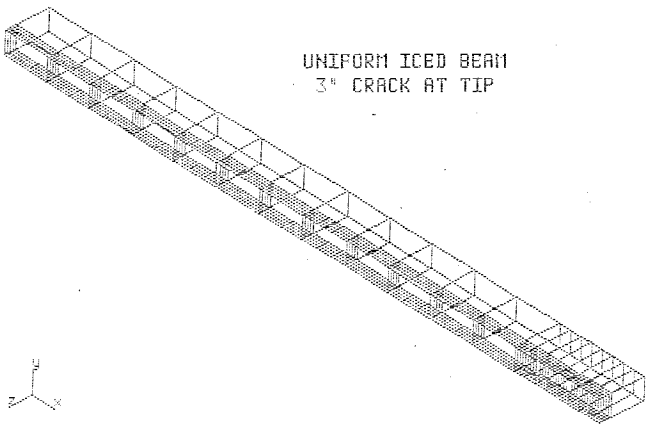

Fig. 6 Finite element model of a uniform continuous iced beam to evaluate shear cracks.

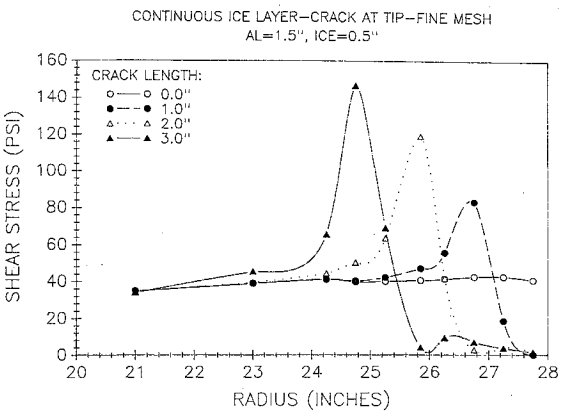

Fig. 7 Calculated shear stresses at the crack tip in a 1.5-in.-thick aluminum beam.

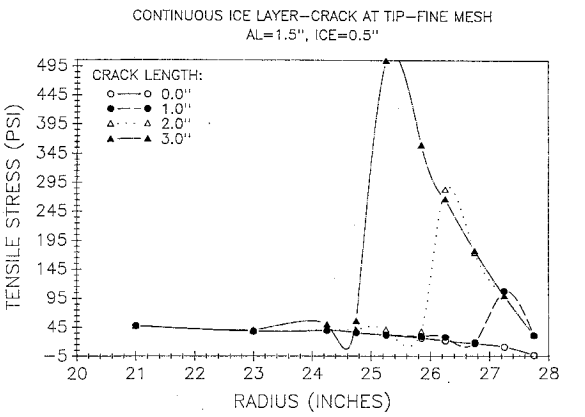

Fig. 8 Calculated tensile stresses at the crack tip in a 1.5-in.-thick aluminum beam.

predicted value of 56 psi for a 0.5-in. ice thickness. After viewing the normal stresses in the ice layer, it is clear that these values are insignificant in magnitude. Obviously, adhesive shear strength is the dominating factor as long as there is continuous adhesion to a relatively rigid airfoil. A summary of the button formula values vs the values calculated by the finite element analyses is found in Table 1. Axial normal stresses in the ice are large for the assumed 0.25-in. aluminum beam. These stresses are caused by both bending and axial strains of the composite structure. However, as the stiffness of the rotating plate is increased, these normal stresses decrease toward zero. For the case that is most stiff, the average normal stress is about 2 psi (Fig. 5).

Shear Crack in a Continuous Ice Layer

The substrate crack finite element model is shown in Fig. 6. This model considers a shear crack developed between a continuous ice layer and the airfoil surface. This model is similar to that of the continuous ice layer model; however, a 4-in.-long fine mesh replaces the original mesh at the end of the beam. Also, particular nodes were numbered twice to enable the ice and beam to be constructed separately from each other and, thus, model a sharp crack at the interface. Figure 7 illustrates the large shearing stress resulting at the tip of the crack. As the crack increases in length, the magnitude of the shearing stress also increases. As is evident from Fig. 8, the normal stress increases from very low values along the ice layer to a level several magnitudes greater than the shear stress at the crack tip. This calculation indicates that, after propagation of a shear crack, a tensile stress failure of the ice will occur. Furthermore, tensile stresses are large enough to cause failure after approximately a 1-in. propagation of a shear crack, assuming the tensile strength of ice to be approximately 100 psi.

Actual Ice Profile on OH-58 Rotor

In order to limit the size of the finite element model, only the outer 5 in. of the rotor and ice were modeled. The inner edge of the ice of this finite element model was assumed free. Based on Saint-Venant's principle, the influence of boundary conditions affects stresses only near the boundary, and resultant stresses away from the boundary are not affected.[13] Thus, stresses at the inner 1 in. of the model are neglected because this apparent strain concentration is caused by the assumption of a free boundary. Stresses are accurately determined away from the boundary. After the modeling technique was refined,[11] and the calculated values were evaluated as being reasonable, an actual ice profile, taken from a model helicopter rotor icing tunnel test, was modeled. The element profile can be viewed in Fig. 9. For this model, it was necessary to include the entire rotor cross section since the ice deposit was not symmetric. It was found that the shear stress varies only a small amount in magnitude in the radial direction (neglecting free boundary conditions), as seen in Fig. 10. The normal stress vs radial position plot, found in Fig. 11, again shows that the normal stress is insignificant for the inner elements and develops a compressive stress at the tip of the rotor.

Many of the tests of the OH-58 rotor were made with large angles of attack. As a result, the next step was to impose a pressure loading on the airfoil. The pressure was calculated using a coefficient of lift that corresponds to an angle of attack of 6 deg. As discussed in Ref. 11, a C_L value of 0.75 was specified. Shear stress results are plotted in Fig. 12. It can be seen that the interface shear stress varies significantly with the radial position. Neglecting the values at the 26-in. radius due to imposed free boundary conditions, the shear stress increased linearly with the radial distance from $R = 27.4$ in. to 30.4 in. There is a slight decrease at the end of the rotor.

Again, the normal stress plotted in Fig. 13 shows the same trend as that of the other models, with values near zero when the end elements are neglected.

Discussion of Results

Itagaki[3] presents one of the few analytical papers on impact ice stresses for rotating airfoils. In this work, it is assumed that tensile stresses and shear stresses act simultaneously. Using this assumption, equations of equilibrium are developed. Tensile and shear stress equations are derived assuming that ice sheds when the centrifugal force in the accreted ice equals the supporting force caused by the combination of shear stresses and tensile stresses. Formulas developed from these assumptions are as follows

$$\tau = \rho\omega^2 hR \tag{2}$$

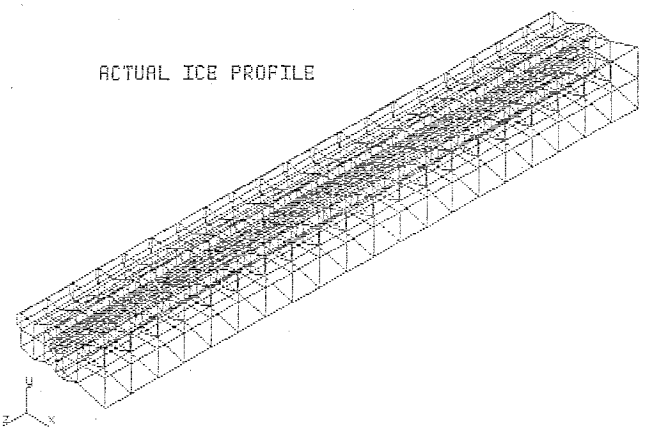

Fig. 9 Finite element model of the last 6 in. of a measured ice profile from the OH-58 test.

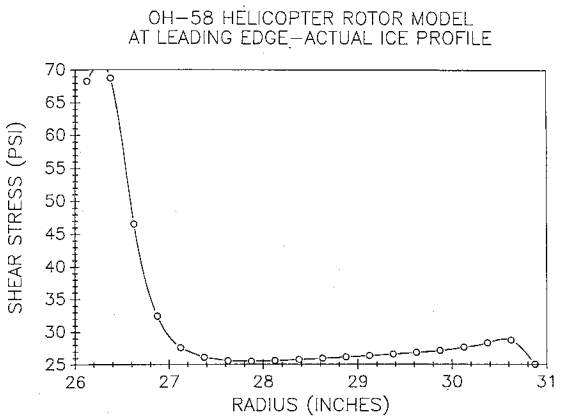

Fig. 10 Calculated shear stresses of the last 6 in. of a measured ice profile from the OH-58 test without lift.

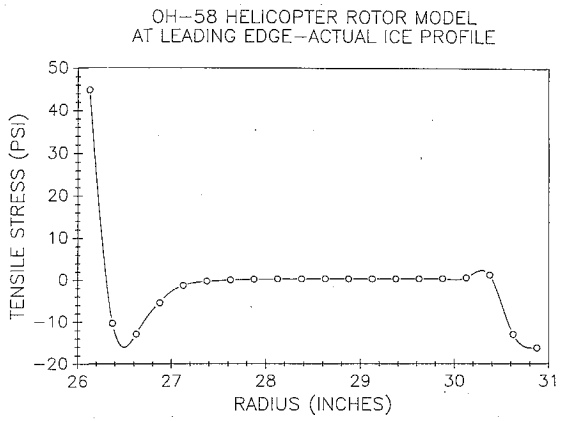

Fig. 11 Calculated tensile stresses of the last 6 in. of a measured ice profile from the OH-58 test without lift.

or

$$\tau = \frac{h\omega\rho(R^2\omega^2\rho - 2\sigma)}{\omega\rho R + \sqrt{2\rho\sigma}} \tag{3}$$

$$\sigma = \frac{\omega^2\rho(R-r)^2}{2} \tag{4}$$

where r is the location of failure surface and R the radius of rotor tensile.

Shear stresses based on the work of Itagaki are plotted in Fig. 14 using the following parameters for the uniform ice layer model: Ω = 2100 rpm = 219.9 rad/s, h = 0.5 in., and R = 28 in. = $8.419*10^{-5}$ lb-s^2/in.^{4}.

As seen in Fig. 14, the tensile stresses almost reach 1600 psi at the center of rotation (radius = 0). The shear stress varies

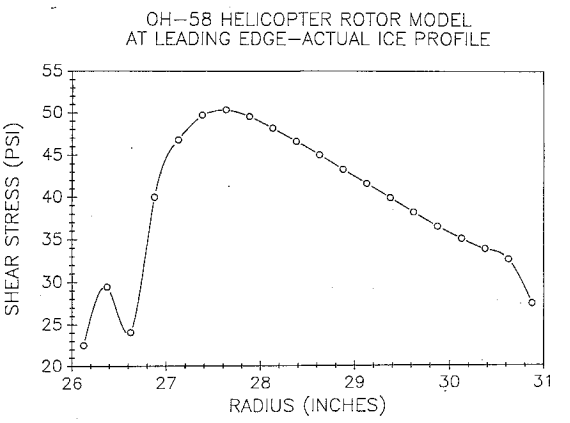

Fig. 12 Calculated shear stresses of the last 6 in. of a measured ice profile from the OH-58 test with lift.

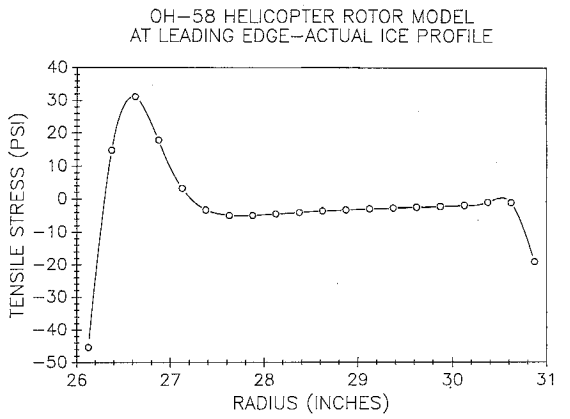

Fig. 13 Calculated tensile stresses of the last 6 in. of a measured ice profile from the OH-58 test with lift.

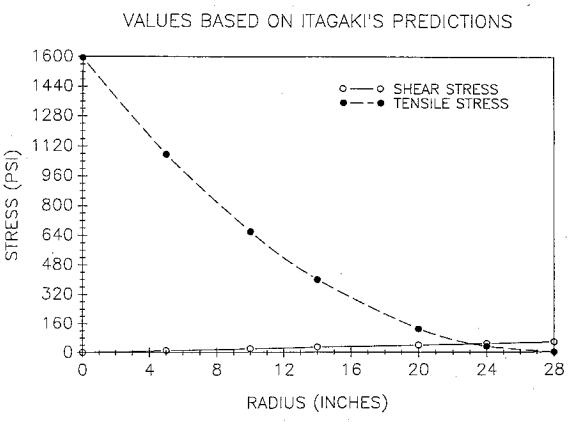

Fig. 14 Calculated shear and tensile stresses based on the work of Itagaki.

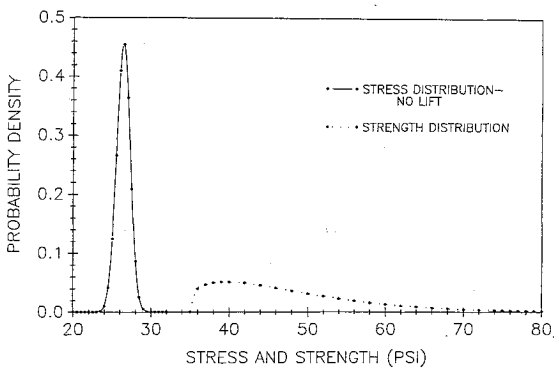

Fig. 15 Stress-strength interaction without lift on the airfoil.

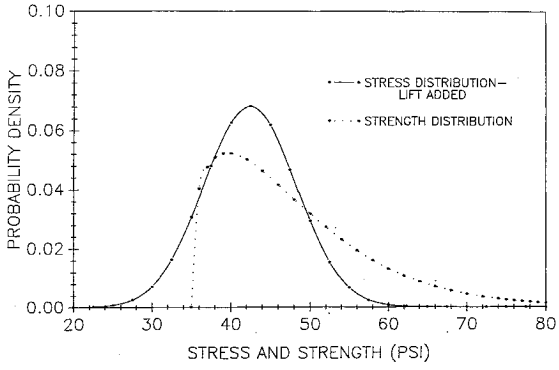

Fig. 16 Stress-strength interaction with lift on the airfoil.

Table 2 Probability of ice shed as mean and standard deviation increase

Mean	Standard deviation	Probability of shed, %
26.4083	0.87277	0
30.0	2.0	0.012
35.0	3.2	5.39
40.0	4.5	24.32
42.9023	5.84846	36.64

from zero at the center to 56 psi at the outer edge. For the rigid airfoil, finite element results indicate that the tensile stresses in the accreted ice approach zero. The reason for this low stress is that the axial strains in the airfoil and ice are approximately equal. Since the modulus of ice is small compared to that of the airfoil and the additional strain caused by the accreted ice mass is also small, tensile stresses in the ice are low as determined from finite element models. However, shear stresses approach the value determined from Eq. (2), which is identical to Itagaki.[3] Eq. (2) can be considered to be an upper bound for a continuous uniform ice layer (Table 1). However, for horned-glaze ice, shear stresses may be underestimated.[11]

Statistical Structural Analysis

A shear stress distribution was calculated for a measured ice profile. By assuming a normal statistical distribution for the calculated shear stress values and using a Weibull distribution for the shear strength distribution (see Ref. 11), a probabilistic combination of the two independent distributions can be utilized to calculate the probability of ice shedding.

The OH-58 data collected by Miller and Bond[6] include ice tracings that are used in the foregoing analysis. An ice tracing that was taken after a run that involved shedding was approximated by finite element analysis. This particular ice shape was taken from a run in which the wind velocity was recorded as 70 mph and droplet size was 15 μ. At this point, it is assumed that the calculated shear stress of ice has a normal distribution.

To find the parameters for this distribution, the shear stress values generated by the finite element analysis for the inside elements at the leading edge were averaged together, and the mean and standard deviation of the shear stress without lift effects were found to be 26.4083 and 0.8728, respectively. As the effects of lift were added to the model by including a pressure load, the mean and standard deviation of the inside elements at the leading edge were calculated as 42.9023 and 5.8486, respectively. The pressure was calculated using a coefficient of lift of 0.75 which corresponds to an angle of attack of 6 deg. The angle of attack used was the average value of the 2 out of 11 cases that shed. The lift coefficient was taken from work done by Potapczuk and Berkowitz[10] on iced airfoils.

It was determined in Ref. 11 that the best fit statistical distribution for the experimental shear strength of ice is the Weibull distribution. From the data collected, the case in which the wind speed was 50 mph and the droplet size was 15 μ best duplicates the conditions of the OH-58 run. There is no definable trend for the shear stress as a function of wind speed on shear stress ice samples, and so no adjustment was made for this difference. Therefore, the parameters for the shear strength data distribution are the following: $S = 47.963$ psi, $\sigma = 10.055$ psi, $x_o = 35$ psi, $b = 1.3027$, and $\Theta = 49.0506$ psi.

Probability of Shedding

The probability of shedding is based on two independent quantities: the shear strength of the ice and the shear stress in the ice. If S denotes the adhesive shear strength of ice and s represents the shear stress in the ice induced by centrifugal force of rotation at the tip of the rotor, then the probability that the ice will not shed is

$$\begin{aligned} P &= P(S > s) \\ &= P(S-s > 0) \\ &= P(y > 0) \end{aligned} \tag{5}$$

where $y = S-s$ = stress difference random variable. Figures 15 and 16 symbolically illustrate the interaction of two independent random variables. The probability of failure or shedding is the probability that the induced stress in the ice is greater than its strength.

By a numerical evaluation of the probability of shedding,[11] the probability that the ice will shed is found to be very close to zero if loading caused by lift is neglected. However, in the case in which lift was taken into account for 6-deg angle of attack, the probability of shedding using the appropriate mean and standard deviation of the calculated stress led to a value of 36.64%. Table 2 shows the relationship between increasing mean and standard deviation to the probability of ice shed. If the calculated stress were reduced from 42.9 to 40 psi, the probability of failure is reduced from 37 to 24%, which is close to the value determined from the OH-58 experimental data.

After examining the OH-58 test data, it was found that 2 out of the 11 test runs in which the actual ice thickness was approximately equal to that modeled by the finite element analysis actually shed ice. The two cases that did shed had angles of attack of 4 and 8 deg. There was no measured ice shedding for zero angles of attack. Therefore, the experimental probability of ice shed is found to be zero when the angle of attack is zero but is calculated as 18.2% when the angle of attack is greater than zero.

Conclusions

Shear stresses in a uniform continuous ice layer are bounded by the button formula and tensile stresses approach zero. When a shear crack propagates at the interface of a uniform ice layer, high tensile stress develops at the crack tip. A tensile failure can be expected after the shear crack propagates to approximately 1 in. in length. Thus, the finite element analysis predicts ice chunks of about 1 in. in length.

When the actual ice formation was analyzed, the stresses calculated approached those expected for a glaze ice formation. Adding lift forces increased the magnitude of shear stress from bending of the composite structure.

The concept of interference can be applied to two random variables of stress and strength of accreted ice to find the probability of shedding. This method appears to be corroborated by the OH-58 experimental results. When the angle of attack is 0 and, hence, there is no lift present, the probability of ice shed was found to be zero both theoretically and experimentally. When the effects of lift were added to the theoretical model and the interference was calculated with a new mean and standard deviation, the probability of ice shed was found to be 36.64%. This value is significantly larger than the OH-58 experimental results (18.2%), although when uncertainty of 10% in the finite element generated stresses is taken into account, the calculated probability of failure is approximately equal to the experimental value.

It should be mentioned that the vibrational effects caused by both the variation of the aerodynamic forces and the unsymmetrical ice loading that constitutes aerodynamic forces imposed on the rotor were not considered. Taking these forces into account would have increased the mean shear stress acting on the ice and, hence, increased the probability of shed. However, the discrepancy between theory and experiment could also be largely attributed to an inadequate number of experimental data points for statistical analysis.

Acknowledgment

The authors would like to acknowledge the support of this work by NASA Lewis Research Center through Grant NAG 3-479.

References

[1]Jellinek, H. H. G., "Adhesive Properties of Ice," U.S. Army, Corps of Engineers, Research Rept. 38, Sept. 1957.

[2]Stallabrass, J. R., and Price, R. D., "On the Adhesion of Ice to Various Materials," National Research Council, Aeronautical Rept. LR-350, NRC No. 6980, Sept. 1963.

[3]Itagaki, K., "Mechanical Ice Release Processes: Self Shedding from High Speed Rotors," Cold Regions Research and Engineering Lab., Hanover, NH, Rept. 83-26, Oct. 1983.

[4]Scavuzzo, R. J., and Chu, M. L., "Structural Properties of Impact Ices Accreted on Aircraft Structures," NASA CR-179580, Jan. 1987.

[5]Druez, J., Clazeau, L., and Tremblay, C., "La Mesure de la Resistance en Traction de la Glaze Atmospherique," *Proceedings of the Eleventh Canadian Congress of Applied Mechanics,* University of Alberta, Edmonton, AB, Canada, June 1987.

[6]Miller, T. L., and Bond, T. H., "Icing Research Tunnel Test of a Model Helicopter Rotor," NASA TM-101978, May 1989.

[7]Lipson, C., and Sheth, N. J., *Statistical Design and Analysis of Engineering Experiments,* McGraw-Hill, New York, 1973.

[8]Duckworth, W. E., *Statistical Techniques in Technological Research,* Methuen, London, 1968.

[9]Bompas-Smith, J. H., *Mechanical Survival, The Use of Reliability Data,* McGraw-Hill, London, 1973.

[10]Potapczuk, M., and Berkowitz, B., "An Experimental Investigation of Muli-Element Airfoil Ice Accretion and Resulting Performance Degradation," AIAA 89-0752, Jan. 1989.

[11]Kellackey, C. J., "The Probability of Ice Shedding from a Rotating Airfoil," M.S. Thesis, Dept. of Mechanical Engineering, Univ. of Akron, Akron, OH, Jan. 1990.

[12]"COSMOS/M User Guide," Structural Mechanics Research and Analysis Corp., Santa Monica, CA, Aug. 1990.

[13]Timoshenko, S. J., and Goodier, J. N., *Theory of Elasticity*, 3rd ed., McGraw-Hill, New York, 1970, p. 39.